International Journal of Pharmaceutics 404 (2011) 220–230

Contents lists available at ScienceDirect

International Journal of Pharmaceutics

journal homepage: www.elsevier.com/locate/ijpharm

Pharmaceutical Nanotechnology

Star-shaped nano-conjugates of cisplatin with high drug payload

Agnieszka Kowalczuk[a], Ekaterina Stoyanova[b], Violeta Mitova[b], Pavletta Shestakova[c,1], Georgi Momekov[d], Denitsa Momekova[d], Neli Koseva[b,*]

[a] Centre of Polymer and Carbon Materials, Polish Academy of Sciences, 34 M. Curie-Sklodowskiej 41-819 Zabrze, Poland
[b] Institute of Polymers, Bulgarian Academy of Sciences, 103 Acad. Georgi Bonchev Str., 1113 Sofia, Bulgaria
[c] Institute of Organic Chemistry with Centre of Phitochemistry, Bulgarian Academy of Sciences, 9 103 Acad. Georgi Bonchev Str., 1113 Sofia, Bulgaria
[d] Faculty of Pharmacy, Medical University of Sofia, 2 Dunav Str., 1000 Sofia, Bulgaria

ARTICLE INFO

Article history:
Received 7 July 2010
Received in revised form 27 October 2010
Accepted 6 November 2010
Available online 13 November 2010

Keywords:
Polymer–drug conjugate
Cisplatin
Star-shaped carrier
Sustained release
Diffusion ordered NMR spectroscopy
Cytotoxicity

ABSTRACT

Core–shell type star polymer bearing carboxylate functions was designed and evaluated as nanocarrier of cisplatin. The synthetic route to the star macromolecules involved the "core first" method to yield a precursor star polymer with a highly branched poly(styrene) core and poly(*tert*-butyl acrylate) arms. Two polymers derived from a common core of M_n = 2400 g/mol and degrees of polymerization of the linear arms 38 and 58 were subjected to acidic hydrolysis to obtain stars with a hydrophilic and multifunctional shell. Diffusion ordered NMR spectroscopic study revealed that the two products presented single populations of stars with values of the apparent hydrodynamic radii 12.9 nm and 14.0 nm, respectively. The stars were loaded with cisplatin via ligand exchange reaction achieving remarkable high drug payload of 45% (w/w). The conjugates were stable in an aqueous solution exhibiting no precipitation for a prolonged period of time. The release profile of the platinum (II) complexes in phosphate buffered saline and RPMI-1640 liquid medium at 37 °C indicated sustained manner of drug release with no initial burst effect. In vitro cell viability study, using four human tumor cell lines proved that the conjugates exhibited lower cytotoxicity compared to the free agent. The established cellular accumulation of cisplatin indicated uptake of the nanoconjugates by the cells through endocytosis.

1. Introduction

Drug conjugation to a macromolecular carrier is a promising strategy especially in the field of cancer therapy. It has been demonstrated that long-circulating polymeric carriers can preferentially and effectively accumulate in solid tumors – a phenomenon known as the "Enhanced Permeability and Retention (EPR) effect" (Matsumura and Maeda, 1986; Maeda et al., 2003). Besides providing passive drug targeting to tumor tissue, polymer–drug conjugates have the potential to increase the therapeutic effectiveness of a drug through optimization of the rate and duration of drug delivery, increasing the solubility of lipophilic drugs or protecting labile agents from chemical or proteolytic degradation. In addition, the release control of highly toxic drugs is as an effective way to minimize their adverse side effects.

Cis-dichlorodiamminoplatinum (II) ($[PtCl_2(NH_3)_2]$, cisplatin) is the most widely used platinum-based antineoplastic agent. It is a potent drug that is usually administered intravenously for treatment of solid malignancies (Sherman and Lippard, 1987). However, a major obstacle to more widespread use of cisplatin is the persistence of severe toxic side effects (Farrell, 1989). Other disadvantages associated with cisplatin clinical use include short circulation period in the blood due to glomerular excretion (LeRoy et al., 1979), intrinsic or acquired resistance of some tumors to the drug and limited aqueous solubility (1 mg/ml) (Wong and Giandomenico, 2000; Ohya et al., 2000).

Cisplatin undergoes ligand exchange reactions kinetics of which is largely determined by the nature of the leaving groups. In biological fluids cisplatin reacts irreversibly with a variety of nitrogen- and sulphur-containing biomolecules (Gullo et al., 1980; Vermorken et al., 1984) that reduce its therapeutic concentration. However, cisplatin also reacts with weaker nucleophiles, i.e. carboxylate ions, and the resulting species are able to undergo the reverse exchange reaction with chloride ions to regenerate cisplatin at physiological salt concentrations (Howe-Grant and Lippard, 1980).

The property of carboxylate ligand as a good leaving group has been exploited to design cisplatin delivery systems based on carboxylate-containing polymers. Polymer–drug complex micelles were spontaneously formed on mixing of cisplatin with PEO-poly(aspartic acid) or PEO-poly(glutamic acid) block copolymers in an aqueous solution (Yokoyama et al., 1991, 1996; Nishiyama et al.,

* Corresponding author at: Institute of Polymers, Bulgarian Academy of Sciences, 103 Acad. Georgi Bonchev Str., 1113 Sofia, Bulgaria. Tel.: +359 2 979 6630; fax: +359 2 870 0309.
E-mail addresses: koseva@polymer.bas.bg, n_koseva@yahoo.co.uk (N. Koseva).
[1] Former family name Denkova.

0378-5173/$ – see front matter © 2010 Elsevier B.V. All rights reserved.
doi:10.1016/j.ijpharm.2010.11.004

1999; Nishiyama and Kataoka, 2001). The cisplatin-incorporated micelles were extremely stable in distilled water whereas in physiological saline the micelles showed dissociation into unimers, accompanied with sustained platinum (II) complexes release. The micelles formed from PEG-b-poly(aspartic acid) underwent fast structural decay (~30 h) that caused liver and spleen accumulation and comparable antitumor activity to free cisplatin despite restrained nephrotoxicity (Kwon et al., 1994). The time scale of decaying of the micelles was prolonged to 50 h when PEO-b-poly(glutamic acid) copolymers were used for cisplatin conjugation which improved the selectivity and efficiency in tumor targeting (Nishiyama et al., 1999).

The metal ligand coordination was also utilized to incorporate the drug into the cross-linked micelles with ionic poly(methacrylic acid) cores and a hydrophilic shell of PEO chains (Bontha et al., 2006). The size of the loaded micelles was about 150 nm and the drug content was determined to be 22% (w/w). Cisplatin was encapsulated in stealth liposomes (Allen et al., 2006; Juñior et al., 2007) and nanoparticles formed by hydrophobically modified chitosan (Kim et al., 2008) or thermosensitive poly(N-isopropylacrylamide-co-acrylamide)-b-poly(D,L-lactide) copolymer (Ding et al., 2007).

In contrast to the particulate carriers such as micelles or liposomes, water-soluble polymers allow drug molecules to interact with a single macromolecule rather than a large particle. The polymer carriers take advantage of EPR effect without accumulating into the liver and spleen. However, linear polymers have limited drug payload capacity. Studies have shown that hyperbranched polymers and dendrimers can carry a higher drug payload due to the large number of tunable surface functional groups (Perumal et al., 2009; Kolhe et al., 2004). A recent patent reported drug payload of 20–25 wt.% for cisplatin loaded polyamidoamine dendrimer with a sodium carboxylate surface (Malik and Duncan, 2003). Besides, dendrimers are well-defined and monodisperse, with a controlled branching architecture but their synthesis is tedious stepwise procedure.

Another alternative are the core–shell type star polymers with hyperbranched cores and the shell of linear polymers with functional groups. These new macromolecules based upon various branched core architectures reveal "unimolecular micelle" behavior in solution, where covalently linked interior and shell parts remain stable independently of concentration, solvent and temperature (Kitajyo et al., 2007). The structural stability, multifunctionality and the presence of cavities in the interior of the stars display potential for conjugation or encapsulation of active compounds (Wang and Lippard, 2005).

Here, we report the synthesis of a new core–shell type star polymer whose interior presents hyperbranched polystyrene bearing arms of poly(acrylic acid). Macromolecular carrier was characterized applying both conventional and diffusion ordered NMR spectroscopy (DOSY). The applicability of the star polymer as cisplatin carrier was explored addressing two challenging aspects: (i) achieving high drug payload, and (ii) evaluating the therapeutic activity of the cisplatin-star polymer conjugates in vitro towards different cancer cell lines. The obtained conjugates were water soluble and carried a 45 wt.% platinum complex payload. The conjugates were also less toxic than cisplatin, displayed sustained drug release and revealed potential as a novel antitumor therapeutic system.

2. Materials and methods

2.1. Materials

p-(Iodomethyl)styrene was synthesized from p-(chloromethyl)styrene via the Finkelstein reaction (Gozdz and Antoni, 1981). *tert*-Butyl acrylate (Aldrich, 98%) was distilled over CaH_2 prior to use. The initiator: α,α′-azobis(isobutyronitrile) (AIBN) (Fluka, >98%) was recrystallized from diethyl ether. Trifluoroacetic acid (Aldrich, 99+%) was used as received. Cis-dichlorodiamminoplatinum (II) (cisplatin) (99.9+%) was purchased from Sigma–Aldrich. Benzene and methanol were purified by distillation at atmospheric pressure. Dichloromethane was used as received. Dialysis membranes with MWCO 1000, 3500 and 1200–1400 were supplied by SpectraPor. Buffer solutions were supplied by POCH SA Poland.

2.2. Synthesis of star polymer with poly[p-(iodomethyl)styrene] core and poly(acrylic acid) arms

The synthesis of the precursor star polymers with poly[(p-iodomethyl)styrene] core and poly(*tert*-butyl acrylate) arms ($PS_{core}PtBuA_{arm}$) was carried out using iodine mediated controlled radical polymerization as described by Kowalczuk-Bleja et al. (2005) yielding copolymers of M_n = 52,000 g/mol and M_n = 77,000 g/mol with average degrees of polymerization of the arms 38 ($PS_{core}PtBuA_{arm}38$) and 58 ($PS_{core}PtBuA_{arm}58$), respectively.

^{1}H NMR (C_6D_6, 300 MHz): δ 1.2–1.6 ppm (CH_3), 1.6–1.9 (CH_2), 3.7–4.7 (CHI and CH_2I), 5.2, 5.9 and 6.3 (CH_2=, –CH=), 6.6–7.4 (CH_{arm}).

The $PS_{core}PtBuA_{arm}$ polymer (1.00 g) was dissolved in 10 ml of dichloromethane. The trifluoroacetic acid in a five-fold molar excess of acid with respect to ester groups was added. The reaction was carried out for 24 h at the room temperature. The precipitated polymer was washed with dichloromethane, dried and dissolved in 10 ml of water. The repeated portion of trifluoroacetic acid was added to the reaction mixture and the hydrolysis was continued for next 24 h. Afterwards the reaction mixture was neutralized using NaOH and dialyzed to remove low molar mass products using SpectraPor membrane with MWCO 1000 g/mol. Subsequently water was evaporated and the obtained product was dried under vacuum. It was assigned as $PS_{core}PA_{arm}$.

^{1}H NMR (D_2O, 600 MHz), δ ppm: 7.2–6.6 (H-atoms from the benzene rings), 2.1–1.7 (C<u>H</u> in the chains) and 1.7–1.0 (C<u>H</u>$_2$ in the chains).

2.3. Loading of star copolymers with cisplatin

Cisplatin was added to an aqueous solution of the star copolymers (2 mg/ml) at pH 9.0 at a molar ratio of cisplatin to carboxylate groups 1:3 followed by stirring of the mixture for 24 h at room temperature. Unbound cisplatin was removed by dialysis against deionized water for 2 days using membrane with MWCO 3500.

For the NMR measurements $PS_{core}PA_{arm}38$ was loaded with cisplatin stepwise by addition of certain amount of the drug to polymer solution in D_2O. During the first step 2 mg cisplatin were added to 1 ml copolymer solution containing 6.5 mg carrier. The mixture was stirred until the initial turbid yellowish solution became transparent and afterwards colorless. At the second and the third step the amount of cisplatin added to the same solution was 1.3 mg and 1 mg, respectively. The feeding ratio [acrylate units]:[cisplatin] was 10:1 at the first loading step, then decreased to 6:1 at the second step and to 4.5:1 after the third addition. At each loading step the system was stirred for 24 h and afterwards ^{1}H NMR and DOSY spectra were measured.

2.4. Platinum (II) complexes release from the loaded stars

The release of platinum (II) complexes from the copolymer carrier in phosphate buffered saline (10 mM PBS, pH 7.4, 0.14 M NaCl) and in RPMI-1640 liquid medium supplemented with 10% fetal bovine serum (FBS) and 2 mM L-glutamine was studied by dialysis

method using a membrane with MWCO 3500. A copolymer solution (4 ml) of known platinum drug concentration was placed into a dialysis tube and dialyzed against phosphate buffered saline (200 ml) at 37 °C and gentle stirring. Aliquots of 10 ml were taken from the solution outside of the dialysis bag at defined time periods and fresh solution of the same volume was added. The concentrations of platinum present in the dialysate aliquots were measured and the concentration of Pt(II) released from the stars was expressed as a accumulative percentage of the total Pt(II) available and plotted as a function of time.

2.5. Analytical methods

2.5.1. NMR spectroscopy

All NMR spectra were measured on Bruker Avance II+ 600 NMR spectrometer using 5 mm direct detection dual broadband probe, with a gradient coil delivering maximum gradient strength of 63 G/cm. The experiments were performed at a temperature of 293 K. ^{1}H NMR spectra were acquired with 32 K time domain points, spectrum width of 9600 Hz and 128 scans. The DOSY measurements were performed with copolymer samples dissolved in KOD/D_2O (pH 9) at concentration of 6.5 mg/ml.

The DOSY spectra were acquired with the double stimulated echo pulse sequence (Jerschow and Müller, 1997), to eliminate possible convection during the experiments. Monopolar smoothed square shaped gradient pulses and two spoiling gradients were used. All spectra were recorded with 16K time domain data points in t2 dimension and 32 t1 increments, 16 transients for each t1 increment, and a relaxation delay of 3 s. Diffusion delay (Δ) of 150 ms and gradient pulse length (δ) of 10 ms were used. The gradient strength G was varied in 32 linear steps from 6 to 95% of the maximum gradient output of the gradient unit to ensure complete signal attenuation. The spectra were processed with an exponential window function (line broadening factor 10) and 16K data points in F2 dimension and 1K data points in the diffusion dimension, using the fitting routine integrated in Topspin2.1 package. The evaluation of the diffusion coefficients was performed by fitting the sum of the columns along the chemical shift of each signal in the DOSY spectrum with the Gaussian distribution curve.

Further, assuming spherical shape approximation the apparent hydrodynamic radius, R_h, of the polymer particles can be estimated using the Stokes–Einstein equation and the obtained value of the diffusion coefficient:

$$R_h = \frac{kT}{6\pi\eta D} \quad (1)$$

where k is the Boltzmann constant, T is the temperature (K) and η is the solvent viscosity. In the present experiment: $\eta(D_2O) = 1.2518 \times 10^{-3}$ Pa s at 293 K (NIST, USA).

2.5.2. Gel permeation chromatography

The molar mass and the dispersity of the precursor polymers with poly(*tert*-butyl acrylate) arms ($PS_{core}PtBuA_{arm}$) was determined by GPC with a differential refractive index detector (Dn-2010 from WGE Dr. Bures) and a multiangle light scattering detector (DAWN EOS from Wyatt Technologies). Measurements were performed using Polymer Standard Service (PSS) columns (SDV 1×10^5 Å, 1×10^3 Å, or 2×10^2 Å) in THF at 35 °C with a nominal flow rate of 1.0 ml/min. The results were evaluated using ASTRA software from Wyatt Technology and WINGPC software from PSS. Refractive index increment (dn/dc) for the poly[p-(iodomethyl)styrene] in THF was 0.205 ml/g (Kowalczuk-Bleja et al., 2004). For poly(*tert*-butyl acrylate) it was measured in THF: $(dn/dc)_{P(t\text{-}BuA)} = 0.055$ ml/g. The refractive index increments for the $PS_{core}PtBuA_{arm}$ copolymer samples were estimated assuming the simple additive relationship: $dn/dc = f_{PS}(dn/dc)_{PS} + f_{P(t\text{-}BuA)}(dn/dc)_{P(t\text{-}BuA)}$, where f_i is the mass fraction of the PS core or P(t-BuA) arms, correspondingly. Where conventional calibration was used, it was established using poly(*tert*-butyl acrylate) (PSS) standards.

2.5.3. Light scattering measurements

Dynamic light scattering (DLS) measurements were performed at 25 °C on a Brookhaven BI-200 goniometer with vertically polarized incident light of wavelength $\lambda = 632.8$ nm supplied by a He–Ne laser operating at 35 mW and a Brookhaven BI-9000 AT digital autocorrelator. Measurements of the scattered light from the aqueous solutions were made at angle 90° to the incident beam. The autocorrelation functions were analyzed using the constrained regularized algorithm CONTIN to obtain distributions of relaxation rates (Γ). The decay rates give distributions of the apparent diffusion coefficients ($D = \Gamma/q^2$), where q is the magnitude of the scattering vector $q = (4\pi n/\lambda)\sin(\theta/2)$ and n is the refractive index of the medium. The apparent hydrodynamic radius is obtained by the equation of Stokes–Einstein (1).

2.5.4. Atom force microscopy

For the atom force microscopy (AFM) analyses, a multimode instrument equipped with a NanoScope 3D controller (MultiMode, Veeco Instruments Inc., USA) operating in tapping mode in air with standard 125 μm single-crystal silicon cantilevers (Model TESP; Veeco Instruments Inc., USA) was used. The piezoelectric scanner had a scan range of approximately 10 μm × 10 μm. The aqueous solutions were spin-coated onto mica wafers in air at 1500 rpm for 8 min. All samples were imaged at room temperature and measured 24 h after coating.

2.5.5. Other analytical methods

Gas chromatography was used to measure the residual monomers content, and p-xylene was used as an internal standard. Measurements were performed on a VARIAN 3400 gas chromatograph with a J&W Scientific DB-5 (30 m × 0.32 mm) column.

The concentrations of platinum (II) present in the dialysate or in the loaded polymer solutions were measured using electrothermal atomic absorption spectrometry (Perkin Elmer AAS Zeeman 3030 with graphite furnace HGA 600) or inductively coupled plasma atomic emission spectroscopy (ULTIMA 2, Jobin Yvon).

2.6. Cell lines and culture conditions

The cell lines used in this study namely HL-60 (acute myelocyte leukemia), K-562 (chronic myeloid leukemia), HUT-78 (T-cell lymphoma) and MDA-MB-231 (breast cancer) were purchased from the German Collection of Microorganisms and Cell Cultures (DSMZ GmbH, Braunschweig, Germany). They were cultured under standard conditions – RPMI-1640 liquid medium supplemented with 10% fetal bovine serum (FBS) and 2 mM L-glutamine, in cell culture flasks, housed at 37 °C in an incubator 'BB 16-Function Line' Heraeus (Kendro, Hanau, Germany) with humidified atmosphere and 5% CO_2. Cell cultures were maintained in logarithmic growth phase by supplementation with fresh medium two or three times weekly.

2.7. Cytotoxicity assessment (MTT-dye reduction assay)

Cellular viability after exposure to free cisplatin or its polymeric formulations (as indicated in Section 3) was assessed using the standard MTT-dye reduction assay as previously described by Mosmann (1983) with some minor modifications (Konstantinov et al., 1999). The method is based on the biotransformation of the yellow tetrazolium dye MTT to a violet formazan product via the mitochondrial succinate dehydrogenase in viable cells. Exponentially growing cells were seeded in 96-well flat-bottomed

Table 1
The characterization of star polymers.

Sample	Precursors: $PS_{core}PtBuA_{arm}$			DP of arm	Hydrolyzed polymers: $PS_{core}PA_{arm}$ M_n calculated[a]
	M_n (GPC-MALLS)[b] (g/mol)	M_w/M_n	M_n (GPC with poly(tBuA) calibration) (g/mol)		
$PS_{core}PtBuA_{arm}38$	52,000	2.30	26,500	38	38,120
$PS_{core}PtBuA_{arm}58$	77,000	1.83	36,000	58	56,920

[a] M_n of the star polymers with arms of sodium salt of poly(acrylic acid) was calculated on the basis of ^{1}H NMR data for the complete hydrolysis of *tert*-butyl acrylate segments.
[b] The refractive index increments were calculated using dn/dc value calculated from the copolymer composition (see Section 2.5.2).

microplates (100 μl/well) at a density of 1×10^5 cells per ml and after 24 h incubation at 37 °C they were exposed to various concentrations of the tested compounds (free or formulated cisplatin) for 72 h or 96 h. For each concentration at least 8 wells were used. After the incubation with the test compounds 10 μl MTT solution (10 mg/ml in PBS) aliquots were added to each well. The microplates were further incubated for 4 h at 37 °C and the MTT–formazan crystals formed were dissolved by adding 100 μl/well 5% HCHO-acidified 2-propanol. The MTT–formazan absorption was determined using a microprocessor controlled microplate reader (Labexim LMR-1) at 580 nm. Cell survival fractions were calculated as percentage of the untreated control. In addition IC_{50} values were derived from the concentration–response curves.

2.8. Data processing and statistics

The cell survival data were normalized as percentage of the untreated control (set as 100% viability). The statistical processing of biological data included the Student's *t*-test whereby values of $p \leq 0.05$ were considered as statistically significant.

3. Results and discussion

3.1. Synthesis of star polymers with a branched poly[p-(iodomethyl)styrene] core and poly(acrylic acid) arms (PSPA)

Star polymers, macromolecules with many arms emanating from a common central point or object, are subject of numerous investigations both because of their unusual behavior in the solution and in the condensed phase, which differs strongly from that of the linear macromolecules, and because of their potential applications e.g. physical incorporation or chemical binding of guest molecules. The synthetic routes to such polymers consist in most cases in the initiation of the living polymerization of arms by a multifunctional initiator ("core first") or by termination of the living polymerization of the arms by a proper multifunctional terminating agent ("arm first").

In this work, the "core first" method was applied as the synthetic route towards star polymers with a polystyrene core and poly(acrylic acid) arms. The procedure included two main steps: (i) the synthesis of precursor star macromolecules with active ester functionalities and (ii) conversion of the latter to carboxylic groups. The star polymers with poly(*tert*-butyl acrylate) arms were synthesized as described previously (Kowalczuk-Bleja et al., 2005) and here only a brief explanation is given for the closer presentation of the structure of the star polymer precursors used in this study.

The core constructing p-(iodomethyl)styrene monomer was polymerized via degenerative chain transfer mechanism using self condensing vinyl polymerization (Frechet et al., 1995; Gaynor et al., 1996), yielding highly branched product of the degree of branching 0.36. The molar mass of the core was determined $M_n = 2400$ g/mol using gel permeation chromatography with light scattering detection (GPC-MALLS). According to the polymerization mechanism every macromolecule contains in its structure one double bond (Gaynor et al., 1996; Weimer et al., 1998) and in average up to 10 active iodomethyl or iodomethine groups. The details are given in Kowalczuk-Bleja et al. (2004). Afterwards, an iodine mediated controlled radical polymerization of the *tert*-butyl acrylate monomer in the presence of the branched polystyrene core was carried out yielding well-defined star polymers. Polymers of $M_n = 52{,}000$ g/mol ($PS_{core}PtBuA_{arm}38$) and $M_n = 77{,}000$ g/mol ($PS_{core}PtBuA_{arm}58$) (Table 1) and monomodal distribution of molar masses have been obtained (Suppl. 1). The star structure of the products has been proven by its hydrodynamic properties (Table 1), where the molar masses from GPC-MALLS evaluation were compared to those based upon the calibration with linear poly(*tert*-butyl acrylate) standards. The much more compact structure of the obtained polymers, as compared with their linear counterparts, supported the star formation.

The second step involved acidic hydrolysis of the linear poly(*tert*-butyl acrylate) arms to polyacids (Fig. 1). The hydrolysis of the ester groups of $PS_{core}PtBuA_{arm}$ polymers in the presence of trifluoroacetic acid proceeded smoothly at the ambient temperature, yielding polymers with a branched hydrophobic interior and hydrophilic shell from poly(acrylic acid) chains. The new polymers are assigned as $PS_{core}PA_{arm}$. The ^{1}H NMR spectra evidence the total removal of the ester groups. The spectrum of $PS_{core}PA_{arm}38$ in the region from 2.8 ppm to 0.2 ppm is presented in Fig. 2a (the entire spectrum is given in Suppl. 2a). It displays two intensive signals in the region 2.1–1.0 ppm that correspond to the CH– and CH_2– fragments from the poly(acrylic acid) chains. The H-atoms of the styrene rings from the hydrophobic core, difficult to be accessed by the solvent, give a broad low intensity signal at about 7 ppm.

Diffusion ordered NMR spectroscopy was used to determine the size of the core–shell type star particles of $PS_{core}PA_{arm}38$ and $PS_{core}PA_{arm}58$ polymers. Diffusion NMR exploits the differences in translational diffusion coefficients of various species present in a mixture, thus allowing discrimination between components with different sizes. Fig. 3a shows the DOSY spectrum of $PS_{core}PA_{arm}38$ in an aqueous solution at pH 9. DOSY spectrum represents a 2D map with chemical shifts of the signals in the horizontal dimension and a logarithm of the diffusion coefficient in the vertical dimension. The top of the 2D spectrum shows the ^{1}H NMR spectrum of the system. The left hand side of the vertical dimension represents the diffusion profile of the studied system, taken as a sum of the columns along the chemical shifts of the signals between 5 and 0.5 ppm. The maximum of the peak in the diffusion profile corresponds to the diffusion coefficient of the respective component (Suppl. 2b).

The DOSY spectrum indicates the presence of one major component at the chemical shifts of the CH_2 and CH groups (1.5–2.5 ppm) of the polymer with diffusion coefficient $D = 1.32 \times 10^{-11}$ m^2/s. Assuming spherical shape approximation the apparent hydrodynamic radius, R_h of the polymer particles can be estimated using the Stokes–Einstein equation (1). The calculated value of the $PS_{core}PA_{arm}38$ stars is $R_h = 12.9$ nm. Similarly, the following values were obtained for $PS_{core}PA_{arm}58$: $D = 1.23 \times 10^{-11}$ m^2/s and

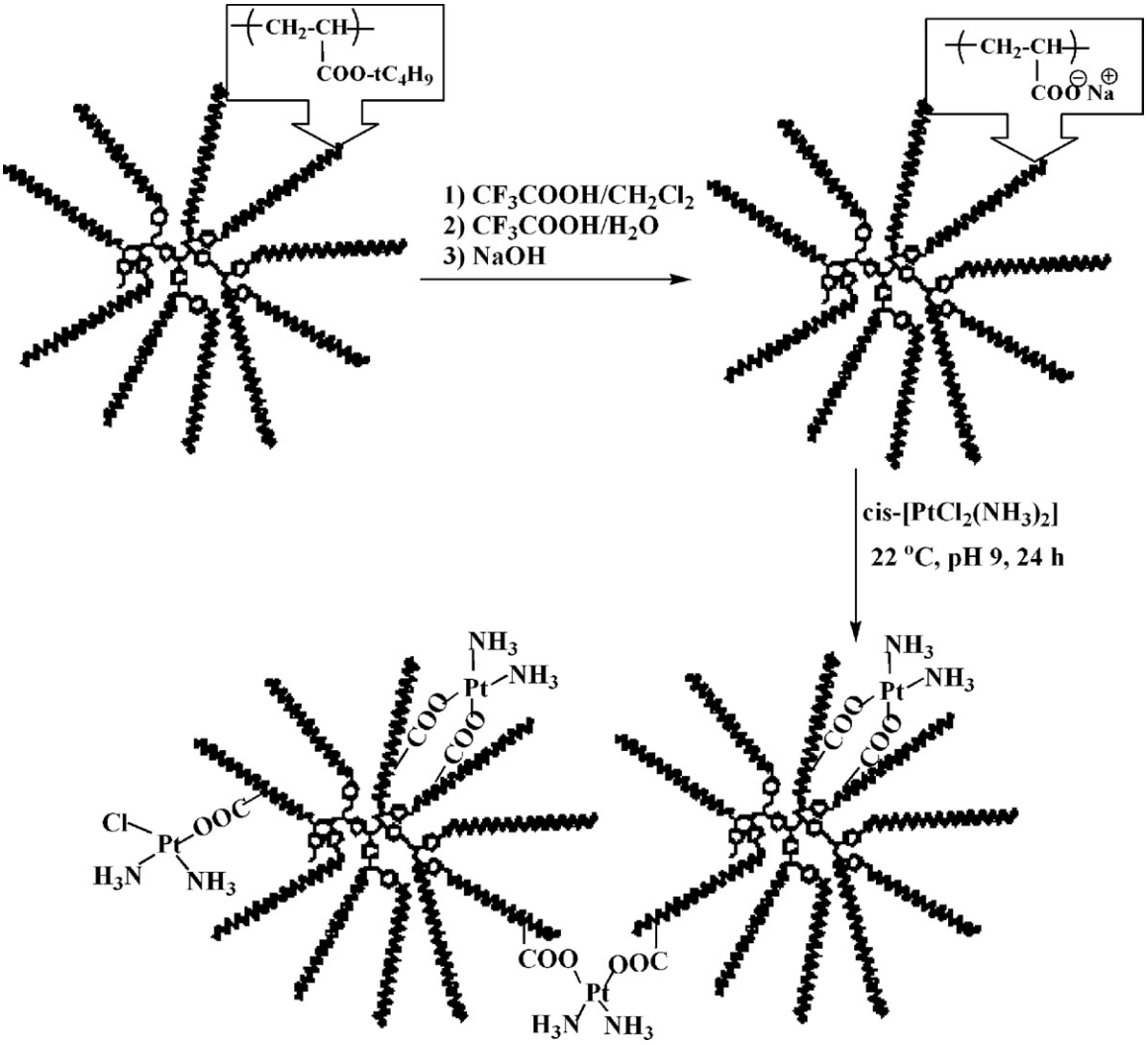

Fig. 1. The route to cisplatin-star polymer conjugates.

R_h = 14.0 nm. In addition to the defined structure of the nanoparticles and the monomodal distribution of their size, the high local concentration of functional groups, i.e. COO^- residues, is an advantageous property for the $PS_{core}PA_{arm}$ polymers to be studied as cisplatin delivery vehicles.

3.2. Loading of star polymers with cisplatin

The star copolymers were loaded with cisplatin by mixing of the aqueous copolymer solution with the drug. The appropriate conditions for cisplatin immobilization in terms of pH, concentration of cisplatin and time of incubation were selected based on a few preliminary experiments and on the results reported by other researchers working in the field (Bontha et al., 2006; Nishiyama et al., 1999, 2001; Nishiyama and Kataoka, 2001; Schechter et al., 1989). Bontha et al. (2006) concluded that polymer micelles with cross-linked poly(methacrylic acid) cores and PEG shells could be saturated with cisplatin for 48 h at pH 9.0 and 37 °C. Having in mind the pK_a value of 4.75 for poly(acrylic acid) (Salamone, 1996; Greenwald and Luskin, 1980) we assumed that the appropriate pH value is above 7 where complete ionization of the carboxylic functions and maximum swelling of the ionic shell of the stars is gained. Upon drug loading changes in the solution properties, i.e. turbidity and color, were monitored by naked eye. The solubility of cisplatin in aqueous media is limited – approximately 1 mg/ml at ambient temperature (Wong and Giandomenico, 2000). Our observations were that at a starting cisplatin concentration in the reaction feed mixture between 1 mg/ml and 2 mg/ml, the turbid yellow mixture became transparent and colorless after 5–10 h stirring at room temperature. These simple observations were an undoubted evidence for drug solubilization through complexation with the macromolecules. Applying an initial cisplatin concentration higher than 2 mg/ml (at the same carboxylate:cisplatin ratio) the solution maintained its turbidity for more than 24 h. Incubation of the mixture at higher temperatures could accelerate the exchange reaction and increase drug solubility but it is known that Pt(II) can undergo a two-electron disproportionation to give solid Pt(0) and soluble Pt(IV) complexes, especially when they are heated in non-acidic solutions (Peleg-Shulman et al., 2001). Therefore, in view of drug stability and time saving the preferred cisplatin concentrations in the reaction mixtures were equal or lower than 2 mg/ml.

Changes of star size and mobility upon drug complexation were followed by NMR measurements. $PS_{core}PA_{arm}38$ was loaded with cisplatin by stepwise addition of certain amount of the drug to the polymer solution in D_2O. The feeding ratio [cisplatin]:[acrylate units] changed as follows: 1:10 at the first loading step, 1:6 at the second step and 1:4.5 after the third addition. The NMR spectra (Fig. 2b–d) clearly indicate broadening of the two signals for CH and CH_2– groups of the polyacrylic arms upon increasing the quantity

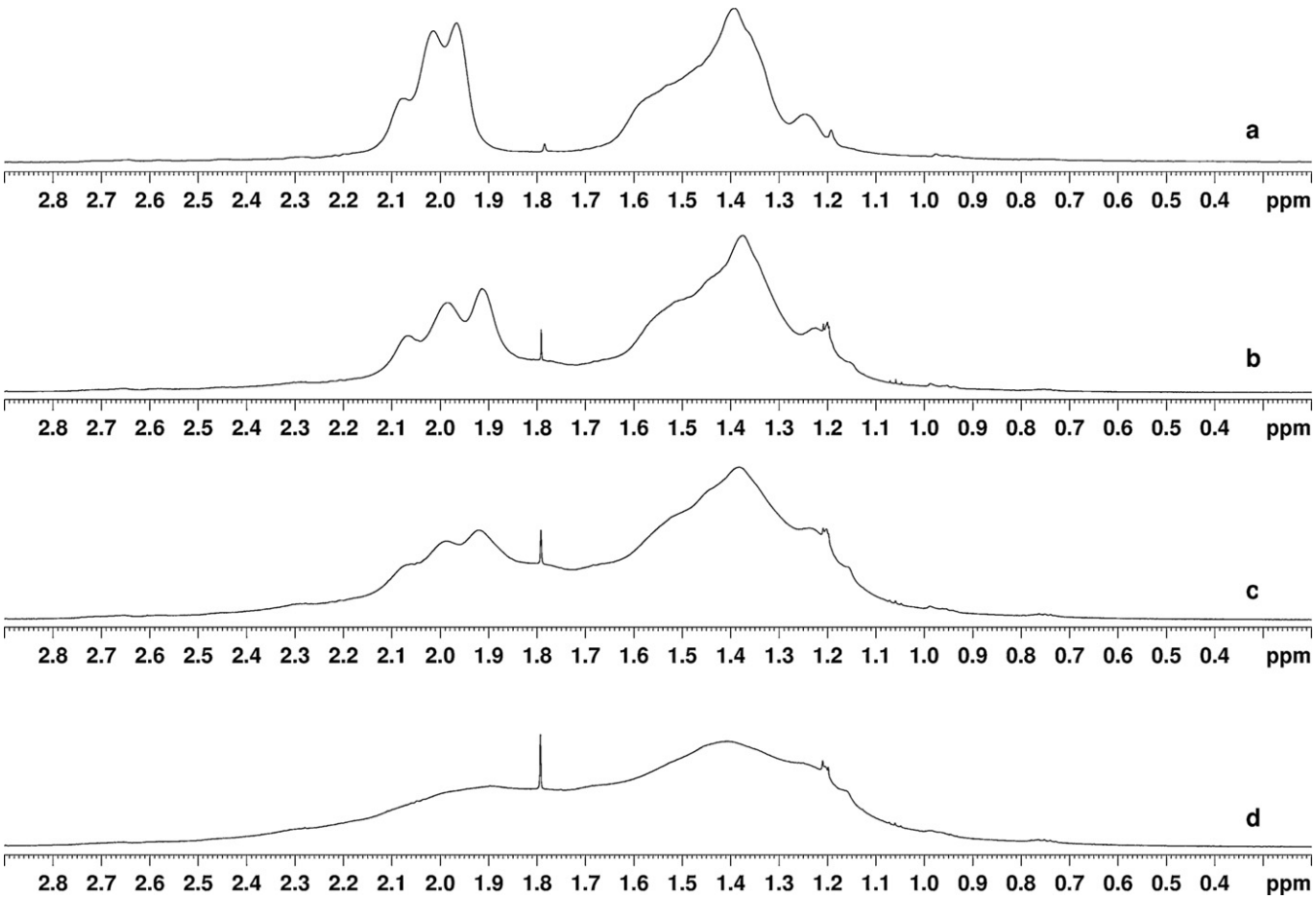

Fig. 2. ^{1}H NMR spectra of the $PS_{core}PA_{arm}38$ star polymer (a) before loading and after step-wise addition of cisplatin to the feed mixture resulting in [acrylate units]:[cisplatin] ratio as follows: (b) 10:1; (c) 6:1; and (d) 4.5:1.

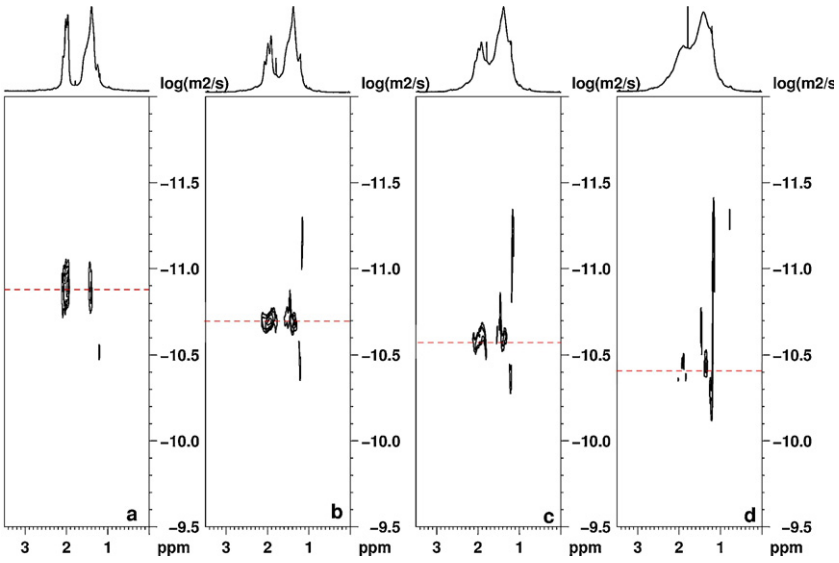

Fig. 3. DOSY spectra of the $PS_{core}PA_{arm}38$ star polymer (a) before loading and after step-wise addition of cisplatin to the feedmixture resulting in [acrylate units]:[cisplatin] ratio as follows: (b) 10:1; (c) 6:1; and (d) 4.5:1.

Table 2
Data about the star copolymer loading with cisplatin in an aqueous solution at a drug concentration of 2 mg/ml, temperature 22 °C, pH 9 and incubation time 24 h.

Sample	Feeding molar ratio [carboxylate]:[cisplatin]	Loading efficiency (%)	Drug mass fraction in the loaded particles (%)
$PS_{core}PA_{arm}38$	3	80	45
$PS_{core}PA_{arm}58$	3	84	46

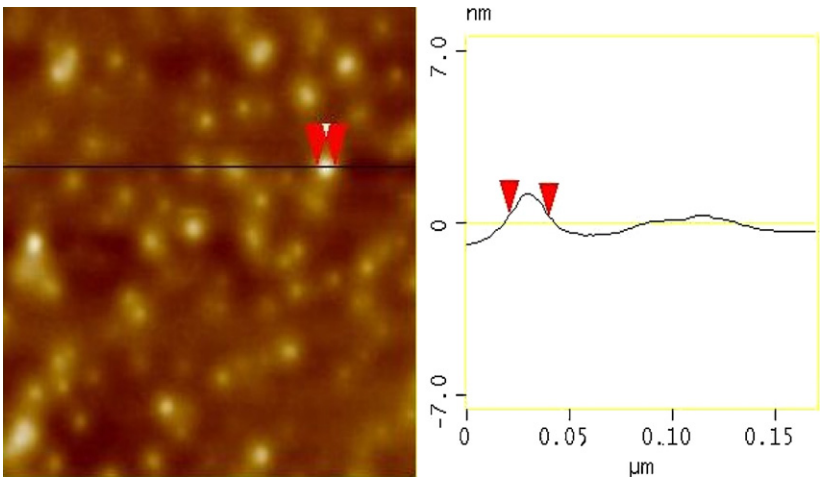

Fig. 4. AFM image of $PS_{core}PA_{arm}58$-Pt conjugate on mica surface.

of the drug. These spectral data evidenced the immobilization of the platinum complex at the coordination sites of the polymer via ligand exchange reaction. The result is reduced chain mobility and signal broadening. Another effect that could contribute to the signal broadening is the formation of some larger particles which most probably are formed as a result of cisplatin induced crosslinking. To further prove this suggestion DOSY spectra were also measured each time after addition of cisplatin to the polymer solution. The results are presented in Fig. 3b–d. The position of the main diffusion peak used to calculate the diffusion coefficient is indicated with a dash line. As already discussed the DOSY spectrum of the polymer shows only one well defined diffusion peak with diffusion coefficient $D = 1.32 \times 10^{-11}$ m^2/s. The results undoubtedly indicate that increasing the quantity of cisplatin leads to an increase of the apparent diffusion coefficient for the main fraction, meaning a decrease of particle size. The measured diffusion coefficients calculated from the DOSY profiles in Fig. 3b–d increase from 2.0×10^{-11} m^2/s to 2.5×10^{-11} m^2/s up to 3.8×10^{-11} m^2/s for the polymer solution with the highest amount of cisplatin. These values correspond to a decrease of particle sizes from 8.6 nm, to 6.8 nm down to 4.5 nm. The only reason for the star contraction could be the binding of cisplatin which lead to a decrease in the negatively charged groups and change in the chain conformation. Similar behavior was detected for polymer micelles with ionic core upon loading with cisplatin (Bontha et al., 2006).

The spectra also display the appearance of slowly diffusing particles upon increase of the amount of cisplatin. The diffusion coefficients calculated for these particles decrease roughly from 7.1×10^{-12} m^2/s to 6.4×10^{-12} m^2/s, down to 5.62×10^{-12} m^2/s at each loading step. Although the trend is well defined the precision of the calculated D values is not very good due to the limiting technical capacity of the used standard NMR gradient equipment. Nevertheless, the results imply that larger particles are also formed in the mixture, which is in agreement with the observed signal broadening in the ^{1}H spectra. The progressive neutralization of the polyacrylic arms due to the binding of cisplatin and the comparatively high polymer concentration could favor star coupling via ligand exchange with drug molecules. The absence of diffusion peaks along the chemical shift lines of the other signals in the DOSY spectrum could be explained with the significant broadening of the signals corresponding to the fragments at the crosslinking sites, due to their immobilization and hence very low signal intensity. However, the solution remained transparent and no precipitation was detected.

Our experimental results and those reported by other researchers point out that the ratio of cisplatin to the coordinating groups of the carrier is an important factor governing the stability of the loaded carrier. For instance, binding of cisplatin to the side chains of poly(L-glutamic acid) through ligand substitution caused precipitation when the molar ratio of drug to L-glutamic acid residues in the polymer exceeded 0.2 (Schechter et al., 1989). Higher molar ratios of the drug to the carboxylate functions were achieved when block copolymers built up from PEG and polycarboxylic chains were used for drug complexing (Nishiyama et al., 2001).

Taking the above into consideration the selected conditions for the drug binding to the star macromolecules were: cisplatin concentration – 2 mg/mL; molar ratio [acrylic units]:[cisplatin] = 3:1; temperature 22 °C; pH 9 and reaction time 24 h. The unbound drug was removed by dialysis against deionized water for 48 h. The obtained conjugates are assigned as $PS_{core}PA_{arm}38$-Pt and $PS_{core}PA_{arm}58$-Pt. Their solutions were colorless and transparent. Under these experimental conditions drug loading efficiency equal or higher than 80% was achieved (Table 2). The corresponding amount of the immobilized cisplatin was determined to be 45% of the mass of the loaded particles.

The size of the loaded nanoparticles was measured in their aqueous solution after dialysis using the light scattering experiment at the angle 90° and polymer concentration of 1.6 mg/ml. The results display one population of particles for the two conjugate solutions and values of the apparent hydrodynamic radius as follows: $R_h^{90^\circ} = 8.7$ nm for $PS_{core}PA_{arm}38$-Pt and $R_h^{90^\circ} = 10.1$ nm for $PS_{core}PA_{arm}58$-Pt. Though the size distribution remained monomodal the dispersity of the particles size (PDI) strongly increased and an average value of PDI = 0.20 was measured for the two conjugates (Suppl. 3). The increase in the size distribution of the stars indicate the formation of larger nanoparticles from stars linked together when COO^- ligands from different macromolecules have reacted with one cisplatin molecule.

The $PS_{core}PA_{arm}38$-Pt and $PS_{core}PA_{arm}58$-Pt loaded particles were visualized by atomic force microscopy (AFM). An AFM image of $PS_{core}PA_{arm}58$-Pt is shown in Fig. 4 (the AFM image of $PS_{core}PA_{arm}38$-Pt is given in Suppl. 4). Spherical in shape particles were observed for the two systems. Their dimensions calculated from the AFM images in horizontal direction are in the range from 17 nm to 23 nm, while in the Z-direction do not exceed 5 nm. Most probably, the observed broadenning in the features could be ascribed to tip convolution effects. Additionally, flattering of the particles caused by electrostatic repulsion between the negatively charged polyacrylate arms of the stars could be also assumed.

It seems that the length of the polyacrylic arms of the stars does not influence the loading capacity of the particles. It is likely

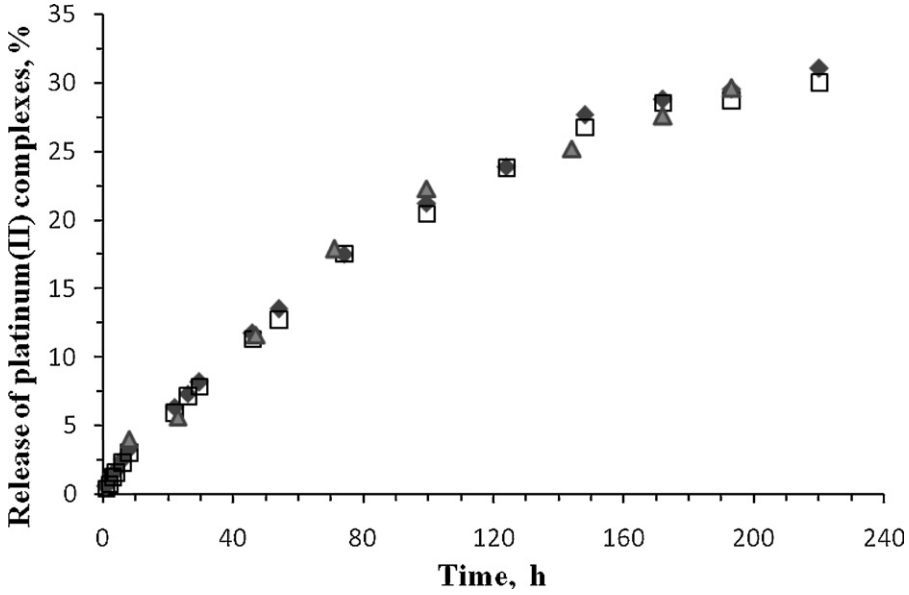

Fig. 5. Release of Pt(II) complexes from drug loaded star copolymers at 37 °C: (♦) $PS_{core}PA_{arm}$58-Pt in phosphate buffered saline (pH 7.4, 0.14 M NaCl); (□) $PS_{core}PA_{arm}$38-Pt in phosphate buffered saline (pH 7.4, 0.14 M NaCl); (▲) $PS_{core}PA_{arm}$38-Pt in RPMI-1640 liquid medium supplemented with 10% fetal bovine serum (FBS) and 2 mM L-glutamine.

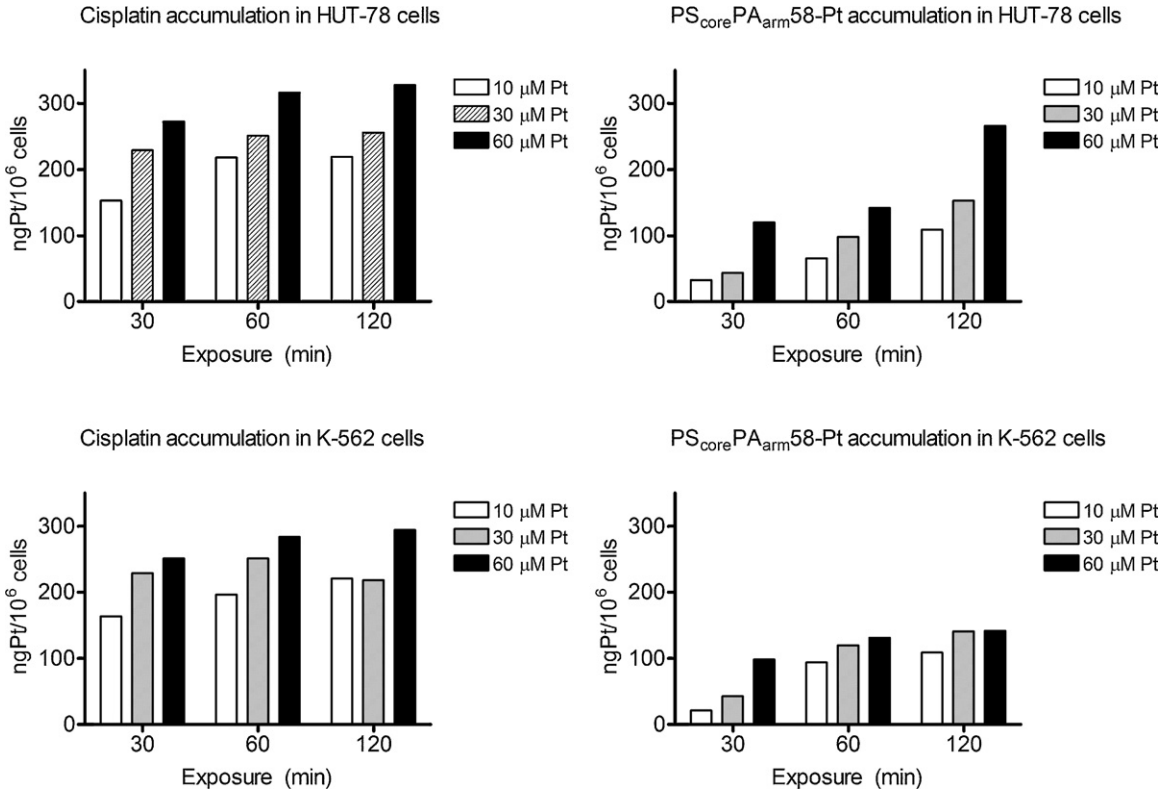

Fig. 6. Intracellular levels of platinum (II).

that the drug molecules could be immobilized through exchange of one or both chloride ligands with carboxylate ions and presumably intramolecular or intermolecular cross-linking through the formation of –COO–Pt–OOC– bridges between acrylic arms may take place (Fig. 1). In addition, the star macromolecules possess comparable or higher loading capacity to the reported in literature carriers (Bontha et al., 2006; Malik and Duncan, 2003) and there is no need to comply with a critical degree of complexation as it was the case with the formation of stable metal–polymer micelles (Nishiyama et al., 1999, 2001). From a pharmaceutical point of view such a remarkably high capacity of drug loading might be considered as a valuable precondition for development of a cisplatin delivery system.

3.3. Release of platinum (II) complexes

The platinum (II) species release from the loaded star macromolecules was evaluated by dialysis method under physiological conditions. The dialysis bags containing a solution of loaded particles with known drug content were immersed in phosphate

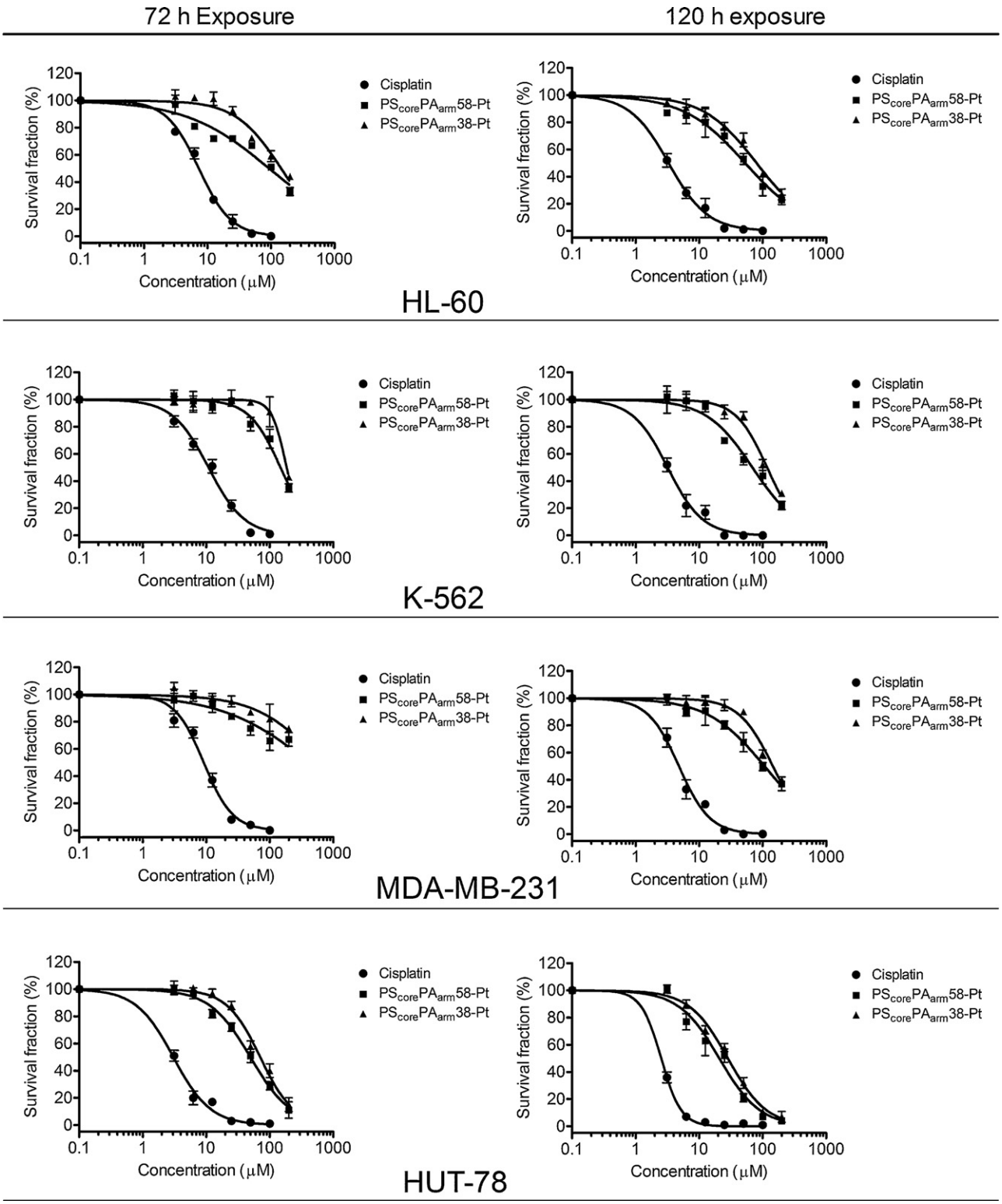

Fig. 7. Cytotoxic effect of (●) free cisplatin; (▲) PS PA 38-Pt and (■) PS PA 58-Pt.

buffered saline (PBS, pH 7.4, 0.14 M NaCl) at 37 °C. The obtained release profiles (Fig. 5) indicate sustain manner of drug release from the macromolecular carrier. One-third of the loaded drug was released within 9 days and no clearly expressed initial burst effect was observed. During the first 8 h of incubation only 4% of the immobilized drug was released. This could be an indication that the whole amount of drug was complexed to the copolymer via ligand exchange. For that reason, no platinum release was evident in distilled water on storage. It was pointed earlier (Bontha et al., 2006; Nishiyama et al., 1999, 2001) that the presence of chloride ions in the physiological solution was essential for the release process, affording conditions for the inverse ligand substitution reaction. Formation of aqua or hydroxo platinum (II) complexes is also possible (Martin, 1999).

An experiment performed in RPMI-1640 liquid medium supplemented with 10% FBS and 2 mM L-glutamine revealed a release profile very close to that obtained in a buffered saline solution. Besides inorganic salts, mainly KCl and NaCl, the RPMI-1640 liquid medium contains variety of amino acids. It is well known that cisplatin and aquachloroplatinum (II) complexes react with sulfur containing amino acids (cysteine, methionine) and proteins thus influencing the ratio between the platinum (II) species (Stefánka et al., 2004; Nagai et al., 1996). Unfortunately, the analytical methods used for determination of Pt content do not differentiate between the platinum (II) species in the solution.

The release of the Pt(II) complexes from both $PS_{core}PA_{arm}38$-Pt and $PS_{core}PA_{arm}58$-Pt conjugates occurred at a similar rate. The increase in the length of the polyacrylic arms influenced insignificantly the release rate of the drug. It is worth mentioning that the observed sustained release of the Pt(II) complexes in physiological saline, also confirmed in RPMI-1640 liquid medium, can be of a great advantage for the passive drug targeting to solid tumors, because of the prolong time periods known to be required for macromolecular drugs to accumulate in solid tumors through the bloodstream (Matsumura and Maeda, 1986).

3.4. Cellular uptake

As the ultimate pharmacological target for cisplatin is the genomic DNA its cellular internalization and hence attaining sufficient intracellular levels is a crucial prerequisite for optimal activity. On this ground we sought to determine whether the polymeric carriers allow intracellular localization of the entrapped drug. To meet this objective exponentially growing K-562 and Hut-78 cells were seeded in sterile Petri dishes and were exposed to cisplatin, as free drug and macromolecular conjugate $PS_{core}PA_{arm}58$-Pt at equimetal concentrations (corresponding to 10, 30 or 60 μM cisplatin) for 30, 60 or 120 min. Thereafter the intracellular levels of platinum were determined using atomic absorption spectroscopy and presented as ng Pt/10^6 cells.

It is evident from the results obtained the free drug was more rapidly and completely internalized by both cell lines, as compared to the corresponding polymer-based formulation of cisplatin (Fig. 6). Nevertheless, the level of platinum uptake was not compatible with the established slow rate of drug release, especially having into consideration the short incubation periods. Hence, the measured cellular accumulation of cisplatin can be ascribed to the uptake of both pre-released complexes and endocytosed drug conjugates.

3.5. Cytotoxicity

In order to evaluate whether cisplatin loaded into the designed nano-carriers exerts cytotoxic effects we carried out an in vitro cell viability study, using a panel of four human tumor cell lines, representative for some clinically important types of neoplastic disease, namely HL-60 (acute promyelocyte leukemia), K-562 (chronic myeloid leukemia), Hut-78 (T-cell lymphoma) and MDA-MB-231 (estrogen receptor-negative breast cancer). Exponentially growing cells were exposed to varying concentrations of free cisplatin and its polymeric formulations (corresponding to 3–200 μM free drug) for either 72 or 120 h. Thereafter, the cellular viability was assessed by the MTT-dye reduction assay and the corresponding IC_{50} values were calculated from the dose–response curves, using non-linear regression analysis.

It is evident from the data presented in Fig. 7 and Table 3 the immobilization of cisplatin in the polymeric nano-carriers results in a shift of the dose response curves to higher concentrations and respectively with an increase of the IC_{50} values. This could be ascribed to the fact that it is the free drug which interacts with DNA to trigger cell death, and hence the established lower cytotoxicity of loaded cisplatin is expected and is consistent with the sustained manner of drug release shown in Fig. 5. Both polymers $PS_{core}PA_{arm}38$ and $PS_{core}PA_{arm}58$ were not toxic at the concentrations used for the conjugates. Nevertheless, by virtue of the EPR effect and the reduced reactivity towards non-pharmacological targets (e.g. serum proteins and low molecular weight thiols), the polymeric conjugates are expected to attain higher intra-tumoral levels of platinum in vivo, as compared to the free cisplatin.

Table 3
IC_{50} values for the free cisplatin and its polymer conjugates.

Cell line	IC_{50} (μmol/l)					
	Cisplatin		$PS_{core}PA_{arm}58$-Pt		$PS_{core}PA_{arm}38$-Pt	
	72 h	96 h	72 h	96 h	72 h	96 h
MDA-MB-23[a]	9.2	4.8	>200.0	107.2	>200.0	145.2
K-562[b]	10.9	3.2	148.3	69.2	185.4	117.9
HL-60[c]	7.3	3.4	94.0	53.3	145.2	80.4
HUT-78[d]	4.1	2.03	49.7	20.9	71.2	28.4

[a] Breast cancer (ER-negative).
[b] Chronic myeloid leukemia.
[c] Acute promyelocyte leukemia.
[d] T-cell lymphoma.

4. Conclusions

A new core–shell nanocarrier was designed as a delivery vehicle of cisplatin. The macromolecules have star geometry with a highly branched core and covalently attached linear arms. These constructs display a combination of key features for drug conjugation, such as hydrophilic shell with high density of functional groups – carboxylate ions that are able to reversibly exchange ligands with cisplatin and therefore to regenerate the agent at physiological salt concentrations. A high drug payload was achieved – higher than the one obtained with the linear homopolymers and alternating copolymers, or dendrimer macromolecules. Diffusion ordered NMR spectroscopy was used to determine the size of the star particles, as well as the changes in their size and mobility upon drug complexation. At the initial stage of cisplatin loading star contraction was monitored. The increase of the drug amount resulted in appearance of larger particles probably due to star coupling via ligand exchange with drug molecules and consequently increase of particle size distribution was observed. However, this cross-linking is reversible in nature under the conditions of drug release. The platinum (II) complexes were released in sustained manner without initial burst effect. In vitro studies reveal lower cytotoxicity of the conjugates consistent with the sustained release of the agent and slower cellular uptake of the conjugated drug compared to that of free cisplatin. Nevertheless, the intracellular levels of platinum (II) complexes indicate that a considerable fraction of the nanoconjugates were endocytosed.

Acknowledgements

The support by the NSF of Bulgaria (Contract No. DO 02-198/2008) and Polish Ministry of Science and Higher Education (Grant No. N N209 100237) is highly acknowledged. The authors are grateful to Dr. Irina Karadjova for the help with ETAAS and ICP AES experiments.

Appendix A. Supplementary data

Supplementary data associated with this article can be found, in the online version, at doi:10.1016/j.ijpharm.2010.11.004.

References

Allen, T.M., Cheng, W.W.K., Hare, J.I., Laginha, K.M., 2006. Pharmacokinetics and pharmacodynamics of lipidic nano-particles in cancer. Anti-Cancer Agents Med. Chem. 6, 513–523.

Bontha, S., Kabanov, A.V., Bronich, T.K., 2006. Polymer micelles with cross-linked ionic cores for delivery of anticancer drugs. J. Control. Release 114, 163–174.

Ding, M.Y.-T., Huang, Z.-Q., Qian, X.-P., Yu, L.-X., Liu, B.-R., 2007. Preparation and characterization of cisplatin-loaded thermosensitive micelle. Chin. J. Inorg. Chem. 23 (2), 205–210.

Farrell, N., 1989. Transition Metal Complexes as Drugs and Chemotherapeutic Agents. Kluwer Academic Publishers, Dordrecht, p. 291.

Frechet, J.M.J., Henmi, M., Gitsov, I., Aoshima, S., Leduc, M.R., Grubbs, R.B., 1995. Self-condensing vinyl polymerization: an approach to dendritic materials. Science 269, 1080–1083.

Gaynor, S.G., Edelmann, S.Z., Matyjaszewski, K., 1996. Synthesis of branched and hyperbranched polystyrenes. Macromolecules 29, 1079–1081.

Gozdz, Antoni, S., 1981. Synthesis and polymerization of p-bromomethylstyrene and p-iodomethylstyrene. Polym. Bull. (Berlin) 4, 577–582.

Greenwald, H.L., Luskin, L.S., 1980. In: Davidson, R.L. (Ed.), Handbook of Water-Soluble Gums and Resins. McGraw-Hill, New York, pp. 17.1–17.19.

Gullo, J.J., Litterst, C.L., Maguire, P.J., Sikic, B.I., Hoth, D.F., Woolley, P.V., 1980. Pharmacokinetics and protein binding of cis-dichlorodiammine platinum (II) administered as a one hour or as a twenty hour infusion. Cancer Chemother. Pharmacol. 5, 21–26.

Howe-Grant, M.E., Lippard, S.J., 1980. Aqueous Platinum (II) Chemistry; Binding to Biological Molecules, Metal Ions in Biological Systems. Marcel Dekker, New York, pp. 63–125.

Jerschow, A., Müller, N., 1997. Suppression of convection artifacts in stimulated-echo diffusion experiments double-stimulated-echo experiments. J. Magn. Reson. 125, 372–375.

Juĭnior, Aĭ.D.C., Mota, L.G., Nunan, E.A., Wainstein, A.J.A., Wainstein, A.P.D.L., Leal, A.S., Cardoso, V.N., De Oliveira, M.C., 2007. Tissue distribution evaluation of stealth pH-sensitive liposomal cisplatin versus free cisplatin in Ehrlich tumor-bearing mice. Life Sci. 80, 659–664.

Kim, J.-H., Kim, Y.-S., Park, K., Lee, S., Nam, H.Y., Min, K.H., Jo, H.G., Park, J.H., Choi, K., Jeong, S.Y., Park, R.-W., Kim, I.-S., Kim, K., Kwon, I.C., 2008. Antitumor efficacy of cisplatin-loaded glycol chitosan nanoparticles in tumor-bearing mice. J. Control. Release 127, 41–49.

Kitajyo, Y., Imai, T., Sakai, Y., Tamaki, M., Tani, H., Takahashi, K., Narumi, A., Kaga, H., Kaneko, N., Satoh, T., Kakuchi, T., 2007. Encapsulation – release property of amphiphilic hyperbranched D-glucan as a unimolecular reverse micelle. Polymer 48, 1237–1244.

Kolhe, P., Khandare, J., Pillai, O., Leih-Lai, M., Kannan, S., Kannan, R.M., 2004. Hyperbranched polymer–drug conjugates with high drug payload for enhanced cellular delivery. Pharm. Res. 21, 2185–2195.

Konstantinov, S.M., Eibl, H., Berger, M.R., 1999. BCR-ABL influences the antileukaemic efficacy of alkylphosphocholines. Br. J. Haematol. 107, 365–380.

Kowalczuk-Bleja, A., Trzebicka, B., Komber, H., Voit, B., Dworak, A., 2004. Controlled radical polymerization of p-(iodomethyl)styrene—a route to branched and star-like structures. Polymer 45, 9–18.

Kowalczuk-Bleja, A., Sierocka, B., Muszyński, J., Trzebicka, B., Dworak, A., 2005. Core–shell polyacrylate and polystyrene-block-polyacrylate stars. Polymer 46, 8555–8564.

Kwon, G., Suwa, S., Yokoyama, M., Okano, T., Sakurai, Y., Kataoka, K., 1994. Enhanced tumor accumulation and prolonged circulation times of micelle-forming poly(ethylene oxide-aspartate) block copolymer–adriamycin conjugates. J. Control. Release 29, 17–23.

LeRoy, A.F., Lutz, R.J., Dedrick, R.L., Litterst, C.L., Guarino, A.M., 1979. Pharmacokinetic study of cis-dichlorodiammineplatinum (II) (DDP) in the beagle dog: thermodynamic and kinetic behavior of DDP in a biologic millieu. Cancer Treat. Rep. 63, 59–71.

Maeda, H., Fang, J., Inutsuka, T., Kitamoto, Y., 2003. Vascular permeability enhancement in solid tumor: various factors, mechanisms involved and its implications. Int. Immunopharmacol. 3, 319–328.

Malik, N., Duncan, R., 2003. Dendritic-platinate drug delivery system. US Patent 6,585,956.

Martin, R.B., 1999. Platinum complexes: hydrolysis and binding to N(7) and N(1) of purines. In: Lippert, B. (Ed.), Cisplatin: Chemistry and Biochemistry of a Leading Anticancer Drug. VHCA, Zurich and Wiley-VCH, Weinheim.

Matsumura, Y., Maeda, H., 1986. A new concept for macromolecular therapeutics in cancer chemotherapy: mechanism of tumoritropic accumulation of proteins and the antitumor agent smancs. Cancer Res. 46, 6387–6392.

Mosmann, T., 1983. Rapid colorimetric assay for cellular growth and survival: application to proliferation and cytotoxicity assays. J. Immunol. Methods 65, 55–63.

Nishiyama, N., Yokoyama, M., Aoyagi, T., Okano, T., Sakurai, Y., Kataoka, K., 1999. Preparation and characterization of self-assembled polymer–metal complex micelle from cis-dichlorodiammineplatinum (II) and poly(ethylene glycol)-poly(alpha,beta-aspartic acid) block copolymer in an aqueous medium. Langmuir 15, 377–383.

Nishiyama, N., Kataoka, K., 2001. Preparation and characterization of size-controlled polymeric micelle containing cis-dichlorodiammineplatinum (II) in the core. J. Control. Release 74, 83–94.

Nishiyama, N., Kato, Y., Sugiyama, Y., Kataoka, K., 2001. Cisplatin-loaded polymer–metal complex micelle with time-modulated decaying property as a novel drug delivery system. Pharm. Res. 18, 1035–1041.

Nagai, N., Okuda, R., Kinochita, M., Ogata, H., 1996. J. Pharm. Pharmacol. 48, 918–924.

Ohya, Y., Shirakawa, S., Matsumoto, M., Ouchi, T., 2000. Design of poly(ethylene glycol) immobilizing platinum complex through chelate-type coordination bond. Polym. Adv. Technol. 11, 635–641.

Peleg-Shulman, T., Gibson, D., Cohen, R., Abra, R., Barenholz, Y., 2001. Characterization of sterically stabilized cisplatin liposomes by nuclear magnetic resonance. Biochim. Biophys. Acta 1510, 278–291.

Perumal, O., Khandare, J., Kolhe, P., Kannan, S., Lieh-Lai, M., Kannan, R.M., 2009. Effects of branching architecture and linker on the activity of hyperbranched polymer–drug conjugates. Bioconjugate Chem. 20, 842–846.

Salamone, J.C. (Ed.), 1996. Polymeric Materials Encyclopedia, vol. 6, M-O. CRS Press, Inc., p. 4086.

Schechter, B., Neumann, A., Wilchek, M., Arnon, R., 1989. Soluble polymers as carriers of cis-platinum. J. Control. Release 10, 75–87.

Sherman, S.E., Lippard, S.J., 1987. Structural aspects of platinum anticancer drug interactions with DNA. Chem. Rev. 87, 1153–1181.

Stefánka, Zs., Hann, S., Koellensperger, G., Stingeder, G., 2004. Investigation of the reaction of cisplatin with methionine in aqueous media using HPLC-ICP-DRCMS. J. Anal. At. Spectrom. 19, 894–898.

Vermorken, J.B., Van der Vijgh, W.J.F., Klein, I., Hart, A.A.M., Gall, H.E., Pinedo, H.M., 1984. Pharmacokinetics of free and total platinum species after short-term infusion of cisplatin. Cancer Treat. Rep. 68, 505–513.

Wang, D., Lippard, J.S., 2005. Cellular processing of platinum anticancer drugs. Nat. Rev. Drug Discov. 4, 307–320.

Weimer, M., Frechet, J., Gitsov, I., 1998. Importance of active-site reactivity and reaction conditions in the preparation of hyperbranched polymers by self-condensing vinyl polymerization: highly branched vs. linear poly[4-(chloromethyl)styrene] by metal-catalyzed "living" radical polymerization. J. Polym. Sci., Part A: Polym. Chem. 36, 955–970.

Wong, E.S.Y., Giandomenico C.M., 2000. Platinum complexes as antitumor agents. US Patent 6,894,049B1.

Yokoyama, M., Okano, T., Sakurai, Y., Ekimoto, H., Shibazaki, C., Kataoka, K., 1991. Toxicity and antitumor activity against solid tumors of micelle-forming polymeric anticancer drug and its extremely long circulation in blood. Cancer Res. 51, 3229–3236.

Yokoyama, M., Okano, T., Sakurai, Y., Suwa, S., Kataoka, K., 1996. Introduction of cisplatin into polymeric micelle. J. Control. Release 39, 351–356.